

DAMPING EFFECT STUDIES FOR X-BAND NORMAL CONDUCTING HIGH GRADIENT STANDING WAVE STRUCTURES*

S. Pei[#], Z. Li, S. G. Tantawi, V. A. Dolgashev, J. Wang, SLAC, CA 94025, U.S.A.

Abstract

The Multi-TeV colliders should have the capability to accelerate low emittance beam with high rf efficiency, X-band normal conducting high gradient accelerating structure is one of the promising candidate. However, the long range transverse wake field which can cause beam emittance dilution is one of the critical issues. We examined effectiveness of dipole mode damping in three kinds of X-band, π -mode standing wave structures at 11.424GHz with no detuning considered. They represent three damping schemes: damping with cylindrical iris slot, damping with choke cavity and damping with waveguide coupler. We try to reduce external Q factor below 20 in the first two dipole bands, which usually have very high $(R_T/Q)_T$. The effect of damping on the acceleration mode is also discussed.

Contributed to the Particle Accelerator Conference, PAC 09, Vancouver, Canada, May 4-8, 2009

*Work supported by the DOE under Contract DE-AC02-76SF00515.
[#] slpei@slac.stanford.edu

DAMPING EFFECT STUDIES FOR X-BAND NORMAL CONDUCTING HIGH GRADIENT STANDING WAVE STRUCTURES*

S. Pei[#], Z. Li, S. G. Tantawi, V. A. Dolgashev, J. Wang, SLAC, CA 94025, U.S.A.

Abstract

The Multi-TeV colliders should have the capability to accelerate low emittance beam with high rf efficiency, X-band normal conducting high gradient accelerating structure is one of the promising candidate. However, the long range transverse wake field which can cause beam emittance dilution is one of the critical issues. We examined effectiveness of dipole mode damping in three kinds of X-band, π -mode standing wave structures at 11.424GHz with no detuning considered. They represent three damping schemes: damping with cylindrical iris slot, damping with choke cavity and damping with waveguide coupler. We try to reduce external Q factor below 20 in the first two dipole bands, which usually have very high $(R_T/Q)_T$. The effect of damping on the acceleration mode is also discussed.

INTRODUCTION

The Multi-TeV colliders should have the capability to accelerate low emittance beam with high rf efficiency, X-band normal conducting high gradient accelerating structure is one of the promising candidate. The long range transverse wake field which can cause beam emittance dilution is one of the critical issues and need to be addressed in the design. The high gradient structures must be efficient in acceleration and effective in damping the high order dipole mode in order to maintain transverse beam stability for multi-bunch operation. We studied dipole mode damping effectiveness with Eigen mode solver Omega-3P in three $a/\lambda=0.14$, X-band, π -mode standing wave structures at 11.424GHz with no detuning considered. They represent three damping schemes: damping with cylindrical iris slot which is a new idea, damping with choke mode cavity such as those used in S and C-band choke mode structures [1, 2] and damping with waveguide coupler similar to that used in CLIC structure [3]. We try to achieve external Q factor below 20 in the first two dipole bands, which usually have very high $(R_T/Q)_T$. Here R_T is the transverse shunt impedance and Q is copper Q-value due to rf losses in copper of the correspondent transverse mode.

In this paper, we present comparisons on the effectiveness of dipole mode damping of these structures. We'll also discuss the effect of the damping geometries on the acceleration mode.

IRIS SLOT STRUCTURE

For all the damping schemes we consider standing wave structures with π phase advance per cell. The power is fed into every one or three cells. We think this will allow us to reach high working gradients based on the

single cell structure test results [4]. Here we describe damping with a slot in the middle of each iris. Figure 1 shows the 4-cell iris slot structure used in our simulation. A slot is located in the center of each iris, which splits each iris into two parts. A dipole mode load made from a cylindrical absorber is located at the outer radius of the slot, in Omega-3P it is set to be pure absorbing boundary condition. 3 mm iris thickness was chosen to incorporate the slot.



Figure 1: 4-cell iris slot structure.

Effect on the acceleration mode

To study the effect on the acceleration mode, especially the surface field, decent meshing was applied to the iris tip. Figure 2 and Table 1 show the results for π -mode in one regular single cell. In the table, R is shunt impedance, E_s is surface field, E_a is accelerating field, Q_0 is quality factor and k is coupling coefficient. It was found that the slot has no big effect on the acceleration mode properties, but the cell to cell coupling increases 10%. The acceleration mode's Q_{ext} is about 10^7 ($<10^8$).

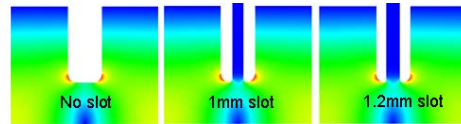


Figure 2: π -mode electric field distribution.

Table 1. Results for π -mode in regular single cell

	No slot	1mm slot	1.2mm slot
Frequency / MHz	11423.87	11423.70	11423.68
R / M Ω /m	87.24	86.42	86.45
E_s / E_a	2.665	2.683	2.739
Q_0	8327	8328	8325
k / %	0.9557	1.0466	1.0533

Dipole mode damping

The E_z field distribution of the acceleration mode on the axis was adjusted to be flat from cell to cell by varying the outer radius of the two end cells. Then the dipole modes' Q_0 , Q_{ext} and $(R_T/Q)_T$ shown in Figure 3 and Figure 4 were calculated for the first two dipole bands by

*Work supported by the DOE under Contract DE-AC02-76SF00515.
[#]slpei@slac.stanford.edu

using quarter model of the 4 cell structure shown in Figure 1 with appropriate boundary conditions. Here Q_{ext} is the dipole mode's external quality factor. The modes in the 3rd dipole band were simulated for structure with no slot and 1mm width slot. Results are shown in Table 2, the 1st and 2nd modes with relatively high $(R_T/Q)_T$ can not be damped well.

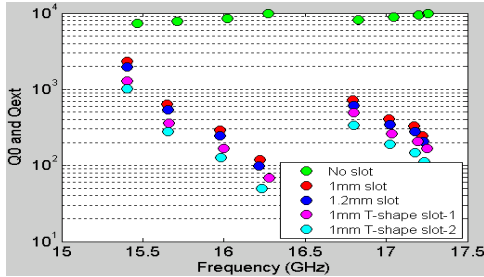


Figure 3: Q_0 (green) and Q_{ext} (others) for dipole modes.

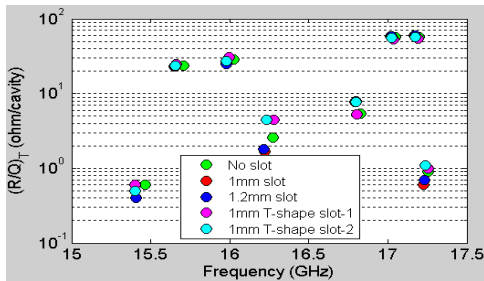


Figure 4: $(R_T/Q)_T$ for dipole modes.

Table 2. Results for dipole modes in 3rd band

	Frequency / MHz	21006	21248	21620	21988
No slot	Q_0	6313	6507	6829	7313
	$(R_T/Q)_T / \Omega/\text{cavity}$	63.56	16.50	16.54	0.50
1mm slot	Frequency/ MHz	20946	21194	21583	21970
	Q_{ext}	9311	1970	605	215
	$(R_T/Q)_T / \Omega/\text{cavity}$	59.16	16.54	7.37	0.54

CHOKE MODE STRUCTURE

Figure 5 shows the 9 cell geometry used in our simulation, which might be different in real case.

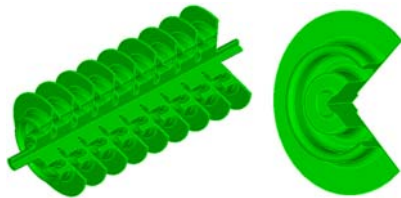


Figure 5: Choke mode structure.

Effect on the acceleration mode

Figure 6 shows the simulation results for single cell choke mode structure. The initial design has 3 mm iris thickness, which is same with that of the iris slot structure. To increase the dipole mode damping, the choke gap width was increased from 1mm to 2.4mm. The iris thickness was decreased from 3 mm to 1.5 mm to compensate part of the shunt impedance reduction. Here, introduction of choke will decrease the shunt impedance by 25% and Q_0 by 5%-15%. Decrease in iris thickness leads to the cell to cell coupling increase by 40% to 50%.

Figure 6: Results for single cell choke mode structure. The figure shows three stages of simulation: 'No choke', 'With choke (initial design)', and 'With choke (optimized design)'. Each stage includes a color-coded electric field plot and associated parameters: frequency, Q_0 , Q_{ext} , R, and k. The 'No choke' stage has 11424.07MHz, $Q_0: 8388$, $R: 83.25\text{Mohm/m}$, and $k: 1.25\%$. The 'With choke (initial design)' stage has 11424.01MHz, $Q_0: 7090$, $Q_{\text{ext}}: 5 \times 10^{11}$, $R: 64.09\text{Mohm/m}$, and $k: 1.14\%$. The 'With choke (optimized design)' stage has 11424.00MHz, $Q_0: 8028$, $Q_{\text{ext}}: 1 \times 10^{10}$, $R: 62.86\text{Mohm/m}$, and $k: 1.76\%$. Between 'No choke' and 'With choke (initial design)', there is a Q drop of 15.5%, R drop of 23.1%, and k drop of 8.8%. Between 'With choke (initial design)' and 'With choke (optimized design)', there is a Q drop of 4.3%, R drop of 24.5%, and k drop of 40.8%. Additionally, there is a Q increase of 13.2% and k increase of 54.4% between the initial and optimized designs.

Figure 6: Results for single cell choke mode structure.

Hybrid structure combining slot and choke

Besides the iris slot and choke mode structures, hybrid structure combining both iris slot and choke cavity shown in Figure 7 was also studied. Here the iris thickness is 3 mm. The effect on the acceleration mode's properties except Q_0 and Q_{ext} is dominated by choke. The acceleration mode's Q_{ext} of hybrid structure is about 10^6 , which is 10 times lower than that of the iris slot structure.

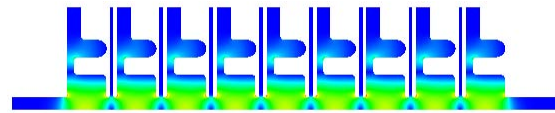


Figure 7: π -mode electric field in hybrid structure

Dipole mode damping

Figure 8 and Figure 9 show the results for Q_0 , Q_{ext} and $(R_T/Q)_T$ of the modes in the first three dipole bands. Hybrid structure has the lowest dipole modes' Q_{ext} 's. However, there is no much benefit because of the lowest acceleration mode's Q_{ext} , which results in extra heating caused by input power leak to the dipole mode load.

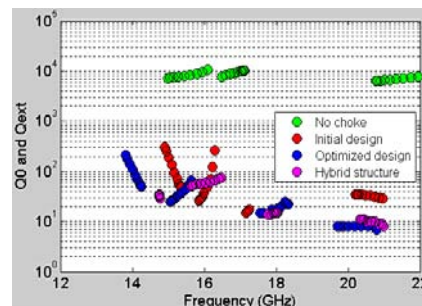


Figure 8: Q_0 (green) and Q_{ext} (others) for dipole modes

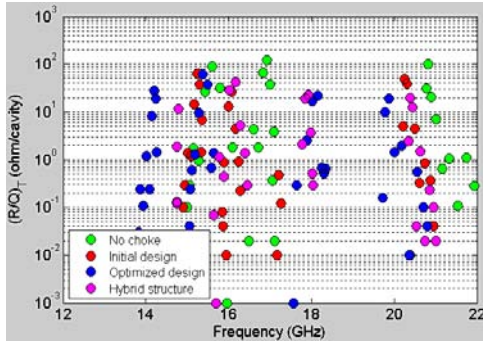


Figure 9: $(R_T/Q)_T$ for dipole modes.

WAVEGUIDE DAMPED STRUCTURE

In the waveguide damped scheme, each cell is coupled to four radial waveguides via coupling irises as shown in Figure 10. Heavy damping of the dipole mode can be achieved with proper design of the iris openings; however this can have significant effects on the acceleration mode and cause reductions of both Q_0 and shunt impedance. The main limiting effect in the waveguide damped structure is pulse heating [5], which can be partially mitigated by optimizing the waveguide and iris opening.



Figure 10: Waveguide damped structure

Effect on the acceleration mode

Table 3 shows the results for π -mode in single cell with 1.5 mm iris thickness. The waveguide and coupling iris used are 11mm \times 2mm and 9mm \times 2mm, respectively. Shunt impedance and Q_0 were reduced by 30% and 25%, which can be recovered back to some extent by further optimization.

Table 3. Results for π -mode in regular single cell

	No damping	Waveguide damping
Frequency/ MHz	11424.16	11424.02
R / M Ω /m	87.01	61.05
Q_0	8921	6636
k / %	2.16%	2.07%

Dipole mode damping

Figure 11 and Figure 12 show the dipole mode damping effect in waveguide damped structures for the first four dipole bands. Almost all of the dipole modes in the second to fourth bands have Q_{ext} lower than 20. For

the dipole modes with high $(R_T/Q)_T$ in the first band, Q_{ext} 's are still lower than 30.

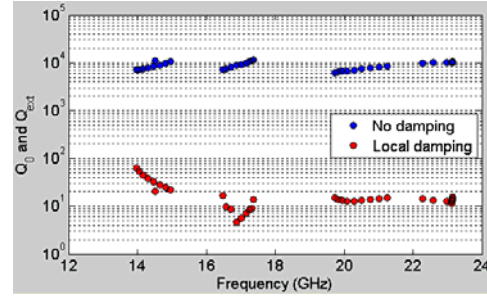


Figure 11: Q_0 (blue) and Q_{ext} (red) for dipole modes

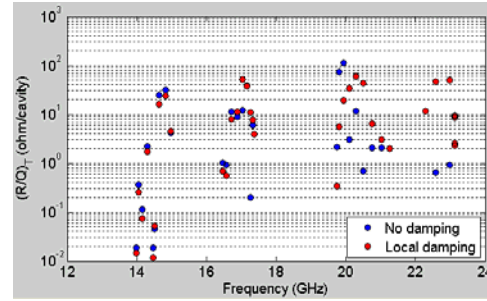


Figure 12: $(R_T/Q)_T$ for dipole modes.

CONCLUSIONS

Three types of damping schemes were studied without considering detuning. For structure with damped iris slot, slot has little effect on the acceleration mode and the lowest Q_{ext} of dipole mode with high $(R_T/Q)_T$ is 100-300. Particular dipole modes in higher band (e.g. 1st and 2nd modes in 3rd dipole band for the 4-cell structure) with relatively high $(R_T/Q)_T$ can not be damped well. For choke structure, with reduction of acceleration mode's impedance by 25% and Q_0 by 5-15%, Q_{ext} 's of most dipole modes with high $(R_T/Q)_T$ s are between 30 and 70, nearly all dipole modes can be damped well. Modes exist in the choke joint with high Q but little effect on beam, which also need to be considered in the design process. waveguide damped structure is the most promising one to reach $Q_{ext} < 20$ for dipole modes, however the waveguide damping scheme increases pulse heating temperature around the coupling irises between cavity and waveguides, which can be mitigated by optimizing the waveguide and coupling iris. To further suppress the dipole modes' effect on beam performance, detuning can be used as well.

REFERENCES

- [1] T. Shintake, Jpn. J. Appl. Phys. Vol. 31, Nov. 1992.
- [2] H. Matsumoto et al. EPAC 96, Jun. 1996.
- [3] I. Wilson et al., LINAC 2000, Aug. 2000.
- [4] V.A. Dolgashev et al. PAC 07, Jun. 2007.
- [5] Z. Li et al. LINAC 2000, Aug. 2000.